Thermoelectric anisotropy and texture of intercalated TiS_2

E. Guilmeau,[a] T. Barbier, A. Maignan, and D. Chateigner
Laboratoire CRISMAT, UMR 6508 CNRS/ENSICAEN, UNICAEN, Normandie Universiti, 6 bd du Maréchal Juin, 14050 CAEN Cedex 4, France

(Received 3 August 2017; accepted 18 September 2017; published online 28 September 2017)

This study addresses the effect of anisotropy on the electrical and thermal properties of Cu_xTiS_2 compounds. We show that the anisotropy of the electrical resistivity ($\rho_{cross\text{-}plane}/\rho_{in\text{-}plane} > 1$) tends to be reduced as the covalent character along c is increased with the Cu content. For all x values ($x \leq 0.1$), the absolute value of S is always found to be higher in-plane than in the cross-plane direction due to band structure anisotropy, leading to higher in-plane power factor values. Interestingly, the $\kappa_{in\text{-}plane}/\kappa_{cross\text{-}plane}$ thermal conductivity ratio, with values similar to the only data reported for TiS_2 crystals, are always higher than $\rho_{cross\text{-}plane}/\rho_{in\text{-}plane}$. This anisotropy relation leads to equivalent zT values for the in-plane and cross-plane directions, reaching 0.35–0.5 at 800 K. *Published by AIP Publishing.* https://doi.org/10.1063/1.4998952

In thermoelectric (TE) materials, anisotropic structures can be essential as in Bi_2Te_3, a long-known TE material with the highest figure of merit zT ($=S^2/\rho\kappa$, where S, ρ, and κ are the Seebeck coefficient, electrical resistivity, and thermal conductivity, respectively) in the T region from room temperature to about 400 K. For the latter, the properties anisotropy is driven by the Te-Te van der Waals interactions along the direction of the atomic layer stacking (c axis). The S values, in-plane (ab) and cross-plane (c), being rather similar, the higher in-plane zT (ab plane) than along c results mostly from the difference in the anisotropies of ρ and κ:[1–3] as $\rho_c/\rho_{ab} > \kappa_{ab}/\kappa_c$ then $\rho_c.\kappa_c > \rho_{ab}.\kappa_{ab}$, explaining why $zT_{in\text{-}plane}$ is higher. TiS_2 is another 2D TE material, the power factor ($PF = S^2/\rho$) measured at 300 K in single crystals is equivalent to that of optimized Bi_2Te_3.[4] However, its TE performances are limited by its too high in-plane κ ($\kappa = \kappa_{el} + \kappa_L$, where κ_{el} and κ_L are for the electronic and lattice part of κ, respectively). Up until now, several routes have been shown to be efficient to reduce κ_L as (self) intercalation or substitution at the Ti or S sites.[5–15] For instance, in crystals, κ_L at 300 K can be reduced by a factor of 5.[9] Although compounds derived from TiS_2 have been the focus of many studies, those concerning the anisotropy of the TE properties are very limited, probably because the platelet-like crystals are usually too thin (typically 20 μm thick, limiting the possibility to measure S_c). For TiS_2 crystals, only 300 K ratios of $\rho_c/\rho_{ab} = 750$ and $\kappa_{ab}/\kappa_c = 1.6$ were reported.[4] As thicker samples are needed for TE applications in TE generators, textured ceramics are usually densified by using Spark Plasma Sintering (SPS).[5–8,10,12,16] However, not much is known about the texture qualification and TE anisotropy for these materials. Only one study of a heavily doped TiS_2 ceramic reported on anisotropic TE properties,[7] with anisotropic S values consistent with the anisotropic band structure,[17] contrasting to the direction quasi-independent values in Bi_2Te_3.[1–3]

This motivated the study of both the texture and anisotropy for a series of Cu_xTiS_2 ceramics exhibiting higher zT values[6] than in Ref. 7. In the present letter, we show that the increasing amount of Cu intercalated between the layers reduces the ρ anisotropy value as the covalent character along c is increased with the Cu content; this covalency is the highest as the atomic number of the $3d$ element increases.[18] For all x values ($x \leq 0.1$), the Seebeck coefficient is also anisotropic with in-plane S values higher than the cross-plane ones, in agreement with the anisotropic band structure. This leads to higher in-plane PF values. Interestingly, in these textured ceramics, the $\kappa_{in\text{-}plane}/\kappa_{cross\text{-}plane}$ ratio, with values similar to the only data reported for TiS_2 crystals,[4] are always higher than $\rho_{cross\text{-}plane}/\rho_{in\text{-}plane}$. This uncommon feature leads to equivalent zT values for the in-plane and cross-plane directions, reaching 0.35–0.5 at 800 K.

The synthesis method of the Cu_xTiS_2 ceramics (x = 0.00, 0.02, 0.05, and 0.10), together with the structural analysis, is described in Ref. 6. Starting from calcined powders with plate-like grains (diameter size of 1–5 μm), the thermomechanical treatment (temperature, time, and uniaxial pressure) during SPS allows simultaneously the growth of the TiS_2 grains (up to 20 μm) and the alignment of plate-like grains (scanning electron microscopy pictures, not shown). The resulting materials are sparsely textured, with their mean c axes parallel to the pressure direction and consequently perpendicular to the pellet surface (for a review, see Ref. 10 and references therein). Note that similar microstructures were observed for all the samples with geometrical densities higher than 95% of the theoretical densities.

In order to obtain a macroscopic view of the texture, by analyzing a larger volume in comparison to scanning electron microscopy, X-ray diffraction analysis has been performed for overall texture determination probing around $\sim 10^6$ crystals. This texture analysis was performed using a 4-circle diffractometer setup equipped with a curved position sensitive detector (CPS120 from Thermofisher Scientific) with monochromatic Cu Kα radiation.[19] Data were processed within the combined analysis formalism implemented in the MAUD software.[20] The sample reference frame is given by the SPS direction of pressure, which corresponds to the centers of the pole figures (Z). Variations of intensities of

[a]Author to whom correspondence should be addressed: emmanuel.guilmeau@ensicaen.fr. Tel.: +33231451367.

the X-ray diffraction diagrams measured for various sample orientations are observed, indicating the presence of a moderately pronounced texture. The combined analysis refinement [Fig. 1(a), $x = 0.05$ sample] correctly reproduces the experimental diagrams, within reliability factors $R_w = 23.19\%$ and $R_{exp} = 17.01\%$. These apparently large values of reliability factors depend on the number of experimental points, which, in the present case, is very large (around 2.3×10^6). From these two factors, a χ^2 value was evaluated to be of 1.6 and corresponds to a good refinement value. The pole figures of the main crystallographic directions of Cu_xTiS_2 samples [Fig. 1(b)] show a moderately strong ⟨001⟩ cyclic-fiber-texture with a nearly 3.6 m.r.d. maximum value of the {001} pole figure. The ⟨001⟩ fiber character of the texture is confirmed by the axially symmetric distribution of the {100} pole figure. The refinement converges to unit-cell parameters and atomic positions close to the already reported values from Rietveld refinements.[6] The overall texture strength, maxima of *OD*, pole figures, and inverse pole figures do not show significant variation with the copper content from X-ray texture analysis. It testifies that copper diffusion and intercalation during SPS has no significant influence on the texturation, i.e., grain growth and alignment. It also confirms the similar microstructures observed for all x contents by scanning electron microscopy.

Such a texturation qualification, generally not reported for TiS_2 and derived ceramics, confirming a similar degree of preferential orientation in the present samples, allows a comparison of anisotropic TE properties to be made (Figs. 2 and 3). All the property measurements were performed on the same pellet (9 mm in thickness and 15 mm in diameter) along the average (*ab*) planes, i.e., in the in-plane direction (perpendicular to the pressure direction) and along the average c axis, i.e., in the cross-plane direction (parallel to the pressure direction). For all sintered compacts, the sign of S and Hall coefficient are negative, which confirms n-type carrier transport. In addition, all compacts show metallic behavior; $|S|$ and ρ increase with temperature. The temperature dependence of the electrical resistivity, ρ, for the four specimens, measured along the in-plane and cross-plane directions (ULVAC-RIKO ZEM3) is shown in Fig. 2(a). As x increases in Cu_xTiS_2, it is found that the ρ values decrease in both measurement directions showing that n-type charge carriers are created by the Cu intercalation.[6] For TiS_2 ($x = 0$) at 300 K, an electron concentration of $n = 6.5 \times 10^{20}\,cm^{-3}$ is measured with a ρ in-plane corresponding value of 1.5 mΩ cm. These values can be well compared to those reported for in-plane measurements in $Ti_{1+x}S_2$ crystals, as for $n = 6.7 \times 10^{20}\,cm^{-3}$, a $\rho_{(300K)}$ value of 0.9 mΩ cm was reported.[21] It demonstrates that the SPS sintering allows obtaining dense and textured specimens so that ρ in-plane is only higher by a factor of 4 than ρ_{ab} of single crystals. The ρ anisotropy is also much lower than in single crystal ($\rho_c/\rho_{ab} = 750$ for TiS_2 in Ref. 4) because, as shown above, the (00*l*) planes are not perfectly

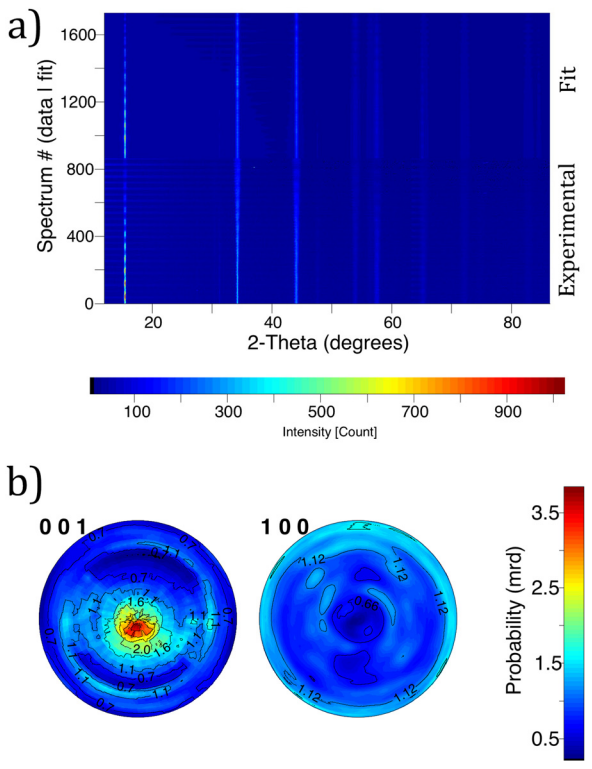

FIG. 1. (a) Evolution of the 2θ diffraction diagrams with the orientation (χ,φ) of the $Cu_{0.05}TiS_2$ sample (vertical scale). The bottom 2D view corresponds to the 864 measured diagrams, developed for increasing (χ,φ) sample orientations (indicated by the diagram numbers), while the top 2D view are the corresponding fits. Note the strong {001} intensity variation ($2\theta \sim 15°$) along (χ,φ) which signs the fiber texture. For clarity, experimental and fit are indicated. (b) Left: {001} and right {100} normalized pole figures reconstructed from the OD. The scale used is logarithmic density scale, equal-area density projections.

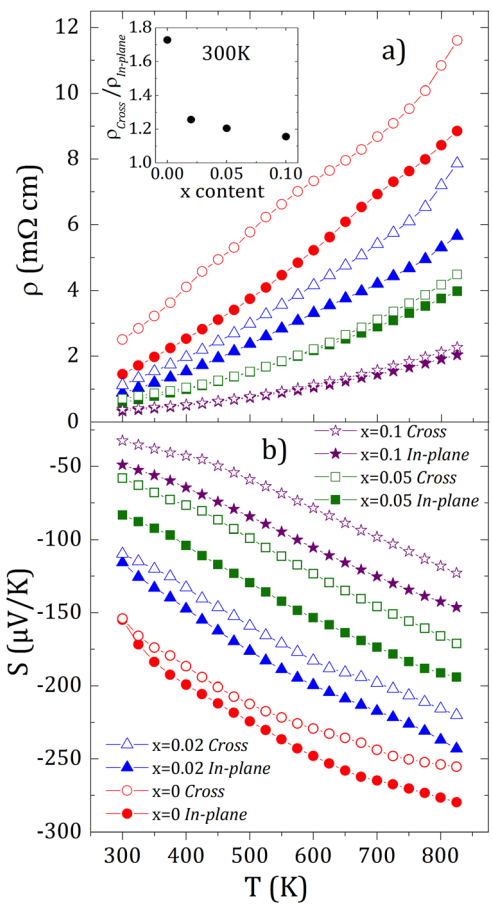

FIG. 2. Temperature dependences of (a) electrical resistivity (ρ) and (b) Seebeck coefficient (S) measured perpendicular (in-plane) and parallel (cross-plane) to the SPS pressing direction in the Cu_xTiS_2 series. The 300 K $\rho_{cross\text{-}plane}/\rho_{in\text{-}plane}$ ratio as a function of x is given as an inset of the top panel.

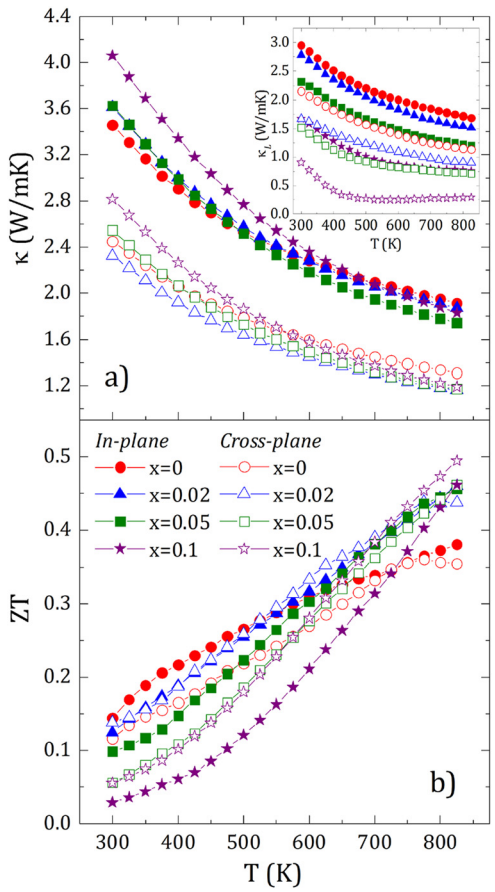

FIG. 3. Temperature dependences of the (a) thermal conductivity (κ) measured perpendicular (in-plane) and parallel (cross-plane) to the SPS pressing direction in the Cu_xTiS_2 series. Lattice thermal conductivities for both directions of measurements are displayed in the inset. (b) Corresponding thermoelectric figure of merit zT as a function of T.

oriented and deviate up to the normal direction. Nevertheless, the anisotropy of the transport properties for the four samples can be well compared since the texture analysis indicated the same degree of orientation in these latter. As expected from the anisotropic crystal structure, the electrical resistivity along the cross-plane direction at the macroscopic scale is around two times higher than along the in-plane direction. It confirms a higher electron mobility ($6.4\,cm^2\,V^{-1}s^{-1}$ at 300 K) in the CdI_2—type layers formed by the TiS_6 octahedra. By plotting the anisotropy factor ρ_c/ρ_{ab} versus x content [inset of Fig. 2(a)], it is obvious that the increasing amount of Cu intercalated between the layers reduces the anisotropic character of TiS_2. Such tendency was addressed in non-stoichiometric (self Ti intercalated) compounds where the anisotropy of the mobility (μ_{ab}/μ_c) was found higher in stoichiometric compounds ($Ti_{1.008}S_2$) than in self-intercalated compounds ($Ti_{1.031}S_2$).[22] It is reasonable to assume that there is a significant interaction between Cu and Ti orbitals, which opens a conduction channel along the c-axis as in Co_xTiS_2.[18] Such an orbital overlap along the c-axis is responsible for the increasing metallic character of ρ_c upon copper intercalation. In 2H-Na_xTaS_2,[23] Fang *et al.* have also shown that the anisotropy of resistivity ρ_c/ρ_{ab} in less intercalated sample ($x \leq 0.05$) is about 60 times higher than that in the more intercalated sample ($x = 0.1$).

The temperature dependence of the Seebeck coefficient drawn in Fig. 2(b) also reveals the existence of a S anisotropy for all Cu_xTiS_2 samples. As x increases, it is found that $|S|$ values decrease, confirming that n-type charge carriers are created by the Cu intercalation. Whereas an insensitivity of S to the crystal orientation (in polycrystalline bulk compounds) was observed by Ohta *et al.*,[22] all our present samples show anisotropic S: the in-plane S values are higher than the cross-plane direction ones. This is in fair agreement with the results reported by Wan *et al.*[7] It suggests probably weaker texture strength in the samples prepared by Ohta *et al.*,[22] as it can be simply assumed by comparing the relative intensities of the diffraction peaks in the respective samples. The (00l) texture strength seems indeed much more pronounced in our samples than those synthesized by Ohta *et al.* On the other hand, the anisotropy of S has been previously reported for the misfit $(LaS)_{1.14}NbS_2$ and $(SnS)_{1.2}(TiS_2)_2$ systems,[7,24] and may arise from the anisotropic band structure due to anisotropic band dispersion of Nb4dz^2 and Ti3d near the Fermi level, in their respective structures. However, anisotropic S properties of single crystals are missing which precludes a definitive conclusion to be made.

Contrasting to the weak and x dependent resistivity anisotropy, the temperature dependence of κ in Cu_xTiS_2 measured along the in-plane and cross-plane directions reveals an unexpected behaviour. κ was obtained from the product of the sample density, heat capacity (Netzsch STA449-F3 *Jupiter*), and thermal diffusivity (Netzsch LFA457) under inert atmosphere from 300 K to 700 K. For all specimens, κ decreases as T increases. The TiS_2 compound ($x = 0$) has a different temperature dependence with comparable or higher κ values (especially over 650 K) as compared to the Cu intercalated compounds. With the increase in x, κ remains rather constant while the lattice part decreases significantly with Cu intercalation [see inset of Fig. 3(a)]. As reported recently by Wan *et al.* in $(SnS)_{1.2}(TiS_2)_2$ misfit layer compounds,[7] the decrease in the lattice thermal conductivity may be linked to the weak interlayer bonding and disruption of periodicity of TiS_2 layers in the direction perpendicular to the layers by the intercalated Cu layers. The Cu intercalation between the TiS_2 layers then generates disorder and phonon scattering even for small Cu content. In addition, the κ values measured in the in-plane direction are higher than those measured along the cross-plane direction, indicating interfacial phonon–phonon scattering that makes the phonon mean free path lower in the cross-plane direction than in the in-plane direction. This effect is linked to the layered structure, but the decrease in κ along the cross-plane direction is also affected by phonon scattering due to a large number of grain boundaries along this direction due to the alignment of plate-like grains. The additional disorder induced by Cu intercalation leads to an extremely low cross-plane lattice thermal conductivity, as shown in the inset of Fig. 3(a). Different from the electrical resistivity anisotropy, the anisotropic factor, κ_{ab}/κ_c, ranges between 1.4 and 1.5, independently of the x content. Thus, it is found that the intercalated species favour phonons scattering in both directions in misfit compounds as suggested by Wan *et al.*.[7]

Combining these physical quantities allows anisotropic zT values to be calculated in the Cu_xTiS_2 series (Fig. 3). Although the four compounds show higher electrical performances

(lower ρ and higher $|S|$) in the in-plane direction, they also show higher κ in that direction. As a result, despite that the in-plane power factor S^2/ρ is the highest, for the cross-plane direction, the combination with κ ultimately produces a zT value similar to the in-plane one. This result demonstrates that, for the level of texture of these Cu_xTiS_2 samples, the Cu intercalation does not allow to increase the zT in a certain direction.

In conclusion, we have characterized the texture and TE anisotropies of Cu_xTiS_2 ceramics densified by SPS. A preferably oriented (00*l*) fiber texture along the pressing direction is obtained for the different samples, which is rather similar with the copper content. It is found that Cu intercalation between the layers inhibits the anisotropic character of TiS_2 due to the formation of conduction paths along the *c*-axis. Differently, the anisotropy of the thermal conductivity is rather independent of the amount of Cu intercalated with the structure. Remarkably, whereas these compounds exhibit superior *PFs* along the in-plane direction, this effect is compensated by the thermal conductivity anisotropy producing similar zT for both directions, contrasting with the behavior reported in Bi_2Te_3. The present zT values achieved for Cu_xTiS_2 ceramics are similar to those reported for the *ab* plane in single crystals. Thus, our main statement is that a weak texturation coupled with a complete densification of TiS_2 compounds is by definition sufficient to achieve thermoelectric performances equivalent to those of single crystals. Finally, this work opens an avenue in the design of 2D materials demonstrating the importance of ceramics to generate performing TE materials.

[1]E. E. Antonova and D. C. Looman, "Finite elements for thermoelectric device analysis in ANSYS," paper presented at the 24th International Conference on Thermoelectrics, ICT, Clemson University, Clemson, SC, USA (IEEE, 2005).
[2]J. P. Fleurial, L. Gailliard, R. Triboulet, H. Scherrer, and S. Scherrer, J. Phys. Chem. Solids **49**, 1237 (1988).
[3]C. Manzano, B. Abad, M. Muñoz Rojo, Y. Koh, S. Hodson, A. Lopez Martinez, X. Xu, A. Shakouri, T. Sands, T. Borca-Tasciuc, and M. Martin-Gonzalez, Sci. Rep. **6**, 19129 (2016).
[4]H. Imai, Y. Shimakawa, and Y. Kubo, Phys. Rev. B **64**, 241104 (2001).
[5]C. Wan, Y. Wang, N. Wang, and K. Koumoto, Materials **3**, 2606 (2010).
[6]E. Guilmeau, Y. Bréard, and A. Maignan, Appl. Phys. Lett. **99**, 052107 (2011).
[7]C. L. Wan, Y. F. Wang, N. Wang, W. Norimatsu, M. Kusunoki, and K. Koumoto, J. Electron. Mater. **40**, 1271 (2011).
[8]M. Beaumale, T. Barbier, Y. Bréard, S. Hébert, Y. Kinemuchi, and E. Guilmeau, J. Appl. Phys. **115**, 043704 (2014).
[9]R. Daou, H. Takahashi, S. Hébert, M. Beaumale, E. Guilmeau, and A. Maignan, J. Appl. Phys. **117**, 165101 (2015).
[10]E. Guilmeau, A. Maignan, C. Wan, and K. Koumoto, Phys. Chem. Chem. Phys. **17**, 24541 (2015).
[11]C. L. Wan, K. K. Gu, F. Dang, T. Ito, Y. F. Wang, H. Sasaki, M. Kondo, K. Koga, K. Yabuki, G. J. Snyder, R. G. Yang, and K. Koumoto, Nat. Mater. **14**, 622 (2015).
[12]T. Sever, M. Maček Kržmanc, S. Bernik, D. Suvorov, and B. Jančar, Mater. Des. **114**, 642 (2017).
[13]M. Beaumale, T. Barbier, Y. Bréard, G. Guelou, A. V. Powell, P. Vaqueiro, and E. Guilmeau, Acta Mater. **78**, 86 (2014).
[14]G. Guélou, P. Vaqueiro, J. Prado-Gonjal, T. Barbier, S. Hébert, E. Guilmeau, W. Kockelmann, and A. V. Powell, J. Mater. Chem. C **4**, 1871 (2016).
[15]F. Gascoin, R. Nunna, E. Guilmeau, and Y. Bréard, J. Alloys Compd. **521**, 121 (2012).
[16]C. Bourgès, T. Barbier, G. Guélou, P. Vaqueiro, A. V. Powell, O. I. Lebedev, N. Barrier, Y. Kinemuchi, and E. Guilmeau, J. Eur. Ceram. Soc. **36**, 1183 (2016).
[17]J. J. Barry, H. P. Hughes, P. C. Klipstein, and R. H. Friend, J. Phys. C: Solid State **16**, 393 (1983).
[18]T. Kawasaki and K. Ohshima, J. Phys. Soc. Jpn. **80**, 044601 (2011).
[19]M. Morales, D. Chateigner, L. Lutterotti, and J. Ricote, Mater. Sci. Forum **408–412**, 113 (2002).
[20]D. Chateigner, *Combined Analysis* (Wiley-ISTE, 2010).
[21]P. C. Klipstein, A. G. Bagnall, W. Y. Liang, E. M. Marseglia, and R. H. Friend, J. Phys. C: Solid State **14**, 4067 (1981).
[22]M. Ohta, S. Satoh, T. Kuzuya, S. Hirai, M. Kunii, and A. Yamamoto, Acta Mater. **60**, 7232 (2012).
[23]C. M. Fang, S. van Smaalen, G. A. Wiegers, C. Haas, and R. A. de Groot, J. Phys.: Condens. Matter **8**, 5367 (1996).
[24]P. Jood, M. Ohta, H. Nishiate, A. Yamamoto, O. I. Lebedev, D. Berthebaud, K. Suekuni, and M. Kunii, Chem. Mater. **26**, 2684 (2014).